AAC Accepts, published online ahead of print on 25 August 2014
Antimicrob. Agents Chemother. doi:10.1128/AAC.02918-14

Phenyl-1-pyridin-2yl-ethanone (PPY)-based Iron Chelators Increase IKBα Expression, Modulate CDK2 and CDK9 activities and Inhibit HIV-1 Transcription

Namita Kumari,[a] Sergey Iordanskiy, [b] Dmytro Kovalskyy,[c] Denitra Breuer,[d] Xiaomei Niu,[a] Xionghao Lin,[a] Min Xu, [a] Konstantin Gavrilenko,[c] Fatah Kashanchi,[b] Subhash Dhawan,[d] Sergei Nekhai[a]#

Center for Sickle Cell Disease, Department of Medicine, Howard University, Washington, DC, USA[a]; National Center for Biodefense and Infectious Diseases, School of Systems Biology, George Mason University, Manassas, VA, USA[b]; ChemBio Center, National Taras Shevchenko University, Kiev, Ukraine[c]; Viral Immunology Section, Laboratory of Molecular Virology, Division of Emerging and Transfusion Transmitted Diseases, Center for Biologics Evaluation and Research, Food and Drug Administration, Bethesda, MD, USA[d]

Running Head: PPY-based iron chelators inhibit HIV-1 transcription

#Address correspondence to Sergei Nekhai, snekhai@howard.edu

Abstract

HIV-1 transcription is activated by Tat protein that recruits CDK9/cyclin T1 to HIV-1 promoter. CDK9 is phosphorylated by CDK2 which facilitates formation of large molecular weight positive transcription elongation factor b (P-TEFb) complex. We showed that chelation of intracellular iron inhibits CDK2 and CDK9 activities and suppresses HIV-1 transcription, but the mechanism of the inhibition was not understood. In the present study, we have tested a set of novel iron chelators for their ability to inhibit HIV-1 transcription and to elucidate their mechanism of action. Novel phenyl-1-pyridin-2yl-ethanone (PPY)-based iron chelators were synthesized and examined for their effect on the cellular iron, HIV-1 inhibition and cytotoxicity. Activities of CDK2 and CDK9, expression of CDK9-dependent and CDK2 inhibitory mRNAs, NF-κB expression and HIV-1 and NF-κB-dependent transcription were determined. PPY-based iron chelators significantly inhibited HIV-1 with minimal cytotoxicity in cultured and primary cells chronically or acutely infected with HIV-1 subtype B, but had less effect on HIV-1 subtype C. Iron chelators upregulated the expression of IKBα with increased accumulation of cytoplasmic NF-κB. The iron chelators inhibited CDK2 activity, and reduced CDK9/cyclin T1 in the large P-TEFb complex. Iron chelators reduced HIV-1 Gag and Env mRNA synthesis but had no effect on HIV-1 reverse transcription. In addition, iron chelators moderately inhibited basal HIV-1 transcription affecting equally HIV-1, Sp1, or NF-kB-driven transcription. By virtue of their involvement in targeting several key steps in the HIV-1 transcription, these novel iron chelators have the potential for the development of new therapeutics for the treatment of HIV-1 infection.

Introduction

HIV-1 transcription is induced by HIV-1 Tat protein (Tat) that recruits CDK9/cyclin T1, the kinase of positive transcription elongation factor b (P-TEFb), to TAR RNA promoting processive elongation of HIV-1 transcription (reviewed in (1)). Basal HIV-1 transcription is activated primarily by host cell Sp1 and NF-kB transcription factors which bind to the HIV-1 long-terminal repeat (LTR) and may also recruit CDK9/cyclin T1 independent of Tat (2). P-TEFb forms a large molecular weight complex (large complex) in which CDK9/cyclin T1 is associated with 7SK RNA and several additional proteins, including hexamethylene bis-acetamide-inducible protein 1 (HEXIM1) dimer, La-related protein 7 (LARP7) protein (3-5), and the methylphosphatase capping enzyme (MePCE) (6, 7). In addition, Tat facilitates the formation of super-elongation complex (SEC) containing active P-TEFb and additional elongation factors and co-activators (8, 9). While the kinase activity of CDK9 in the large P-TEFb complex is suppressed (10, 11), this complex serves as the source of CDK9/cyclin T1 for the recruitment by HIV-1 Tat (12). In a recent study, we have demonstrated that HIV-1 transcription is regulated by CDK2 that phosphorylates the Ser90 amino acid residue of CDK9 (13). Dephosphorylation of this residue reduces the P-TEFb large complex and decreased HIV-1 transcription (13). Macrophages differentiated from induced pluripotent stem cells with stable CDK2 knock-down also exhibited the reduced susceptibility of these cells to HIV-1 infection (14), confirming our previous observations of CDK2 as a key regulator of HIV-1 transcription.

We have previously described a role of iron chelators in the inhibition of HIV-1 transcription and replication by likely reducing the activities of CDK2 and CDK9 (15, 16); however, the exact mechanism of action has remained unclear. Induction of p21 (CIP1/WAF1) expression by iron

chelators has recently been shown to inhibit CDK2 activity in 293T cells (17-19). Moreover, blocking of p21-mediated CDK9 and viral reverse transcriptase activities provide a potential protection barrier against HIV-1 infection (17). Since CDK2 phosphorylates the HIV-Tat protein and also the host protein CDK9 (18), it may be possible that the induction of p21 by iron chelators could inhibit the CDK2 activity leading to the suppression of CDK9-dependent HIV-1 transcription (19). HIV-1 Tat also recruits NF-κB along with CDK9/cyclin T1 (2) and this recruitment occurs in a cooperative manner (20, 21) as Tat interacts with the p65 subunit of NF-κB through NFBP protein (22). HIV-1 basal transcription is largely regulated by the Sp1 transcription factor (23) which recruits CDK9/Cyclin T1 to the LTR in the absence of Tat (24). Tat also stimulates Sp1 phosphorylation by DNA-PK, which also contributes to the induction of HIV-1 transcription (25).

In the present study, we thought to further analyze the mechanism of HIV-1 inhibition by iron chelators using several novel iron chelators which had flexible scaffold that as compared to the previously reported DpT and BpT-based chelators (15). We created novel phenyl-1-pyridin-2yl-ethanone (PPY)-based iron chelators which were analyzed for HIV-1 inhibition. The iron chelators efficiently reduced cellular iron and also hampered cell cycle progression of the treated cells. The chelators inhibited HIV-1 subtype B infection in cultured and primary cells and also in the chronically infected T cells at low or sub nanomolar concentrations without being cytotoxic. The chelators efficiently reduced HIV-1 mRNA expression but had no effect on reverse transcription. We observed increased expression of p21, cyclin A and cyclin E, and increased G1 cell cycle accumulation of the T cells treated with iron chelators. Iron chelators inhibited CDK2 activity and also reduced CDK9/cyclin T1 in the large P-TEFb complex. Analysis of CDK9-

dependent genes showed increased expression of NF-κB inhibitor, IKBα. In the cells treated with iron chelators, NF-κB was found accumulated in the cytoplasm and the overall expression level of NF-κB was decreased. Iron chelators had more profound effect on Tat-activated HIV-1 transcription than on basal HIV-1, Sp1 or NF-kB-driven transcription. Our results indicate that PPY-based iron chelators markedly inhibit HIV-1 transcription by inhibiting CDK2 and CDK9 activities that were directly related to the upregulation of p21 expression and down regulation of NF-κB expressions via the IKBα induction mechanism.

Materials and Methods.

Cells and media. 293T, THP1 and CD4+ T cells (CEM) were purchased from the American Type Culture Collection (Manassas, VA). J1.1 and A3R5.7 cell lines were from NIH AIDS Research and Reference Reagent Program. PBMCs were purchased from Astra Biologics. All cells were cultured at 37°C in a 5% CO_2 atmosphere. CEM and chronically HIV-1 infected J1.1 T cells as well as promonocytic THP1 cell line were cultured in RPMI 1640 medium (Invitrogen, Carlsbad, CA) containing 10% fetal bovine serum, and 1% antibiotic solution (penicillin and streptomycin; Invitrogen). Human T lymphoblastoid cell line A3R5.7 expressing CD4, CXCR4 and CCR5 receptors was cultured in the complete RPMI-1640 medium supplemented with Geneticin (G418, 1mg/ml) The 293T cells were cultured in Dulbecco's modified Eagle's medium (Invitrogen) containing 10% fetal bovine serum and 1% antibiotic solution (penicillin and streptomycin).

Plasmids. The HIV-1 proviral clone NL4-3 (26) was kindly provided by Prof. Lee Ratner. The

HIV-1 subtype C proviral clone HIV1084i (27) was a kind gift of Prof. Charles Wood. HIV-1 proviral vector pNL4-3.Luc.R$^-$E$^-$ (courtesy of Prof. Nathaniel Landau, NYU School of Medicine, New York, NY) was obtained from the NIH AIDS Research and Reference Reagent Program. HIV-1 LTR luciferase expression vectors were kindly provided by Dr. Manuel López-Cabrera (Unidad de Biología Molecular, Madrid, Spain) (28): HIV-1 LTR (-105 to +77) followed by the *luciferase* reporter gene (HIV LTR 2xNFκB 3xSP1); HIV-1 (-105 to +77) with Sp1-inactivated sites followed by the *luciferase* reporter gene (HIV LTR 2xNFκB ΔSP1); and HIV-1 (-81 to +77) with NF-κB-deleted sites followed by the *luciferase* reporter gene (HIV LTR ΔNFκB 3xSP1).

Antibodies. Antibodies for IKBα, IKBα phosphorylated on Ser32 (IKBα-P), NF-κB p65 subunit and p21 were purchased from Cell Signalling Technology (Danvers, MA). Antibodies for α tubulin were from Sigma. Antibodies for p21 were from BD Biosciences.

Synthesis of PPY (2-phenyl-1-pyridin-2yl-ethanone). Previously described Bp4eT and Bp4aT tridentate iron chelators (Fig.1A) were modified by substituting phenyl group with the benzyl moiety. The general steps for the synthesis of PPY compound are shown in Fig.1B. A solution of phenylacetonitrile (23.4 g,0.2 mol) and methyl picolinate (30 g, 0.22 mol) in 100 mL of tetrahydrofuran (THF) was added dropwise into suspension of NaH (16.8 g, 0.42 mol, 60%w in parafine) in 300 ml of THF while stirring and cooling in an ice-water bath. Reaction mixture was stirred and cooled with water bath additionally 2 hours. Then a water bath was removed and the reaction mixture was stirred overnight at RT, Next day dark solution was evaporated under reduced pressure and solid residue was dissolved in a minimal amount of water and extracted

twice with 200 mL chloroform. The water layer was acidified with concentrated hydrochloric acid (300 mL) and refluxed one day, cooled down to RT and leave at RT for overnight. Ahydrochloride precipitate was filtered, washed with acetone, and air-dried. The hydrochloride salt was dissolved in 100 ml methanol. Sodium hydrocarbonate was added in portions with stirring until production of gas stopped and the mixture was further stirred for 30 min. The solution was then filtered and evaporated. The obtained solid residue was treated with 50 ml water and 100 ml chloroform. The organic layer was removed, and the water layer was extracted with 100 ml chloroform. The combined chloroform solution was dried over anhydrous sodium sulphate and evaporated. After complete crystallization, the product was washed with a small amount of cold hexane, and air-dried. PPY was isolated in 9.8 g.

Synthesis of PPYeT and PPYaT. An equimolar mixture of the PPY (2.5 mmol) and appropriate thiosemicarbazide was refluxed in 20 ml of 1:1 water-ethanol mixture for 24 hours. After cooling, a precipitated product was filtered off and dried under vacuum at 60ºC.

PPYeT was isolated in 0.42 g (56% yield).

PPYaT was isolated in 0.56 g (72% yield).

LC-MS analysis of PPY-based compounds. PPY, PPYeT and PPYaT were dissolved in DMSO to prepare stock solutions (10 mM), which were further diluted to 100 µM with 0.1% formic acid aqueous solution for nano LC-FTMS analysis. The samples were loaded to nano C18 column attached to Shimadzu nano LC coupled in-line to LTQ Orbitrap XL tandem mass spectrometer (Thermo Fischer Scientific, GA, USA). The injection volume was 0.2 µL. The mobile phase consisted of a 0.1% formic acid aqueous solution (A) and a 0.1% formic acid

acetonitrile solution (B). The gradient elution program was as follows: 0–6.02 min, 1% B; 6.02–6.11 min, 1–2% B; 6.11–10 min, 2−98% B; 10–30 min, 98 B% (v/v). The flow rate was set at 600 nL/min. The compounds were ionized by electrospray ionization and detected by Orbitrap at 30000 mass resolution (full scan, *m/z* 180-2000). The spray voltage, capillary temperature and capillary voltage were set to 2.0 kV, 200 °C, and 39.5 V, respectively.

Determination of the effect of iron chelators on labile iron pool (LIP). The effects of PPY-based iron chelators on the labile iron pool (LIP) in human acute monocytic leukemia (THP-1) cells was examined as described previously (29). Cells were loaded with Calcein-AM, a non-fluorescent, hydrophobic compound that easily permeates intact, viable cells. Treatment of the cells with iron chelators removes the calcein-bound iron and produces Calcein, a hydrophilic, strongly fluorescent compound that is well-retained in the cell cytoplasm. The fluorescence intensity is related to the amount of cellular iron that had been effectively removed by the chelators (29). The chelating efficiency was quantified using the formula: $(F-F_0)/F_0$, where F_0 = the fluorescence intensity in the presence of chelator at time 0 and F = the fluorescence intensity at a given time after the addition of the chelator. The values derived from $(F-F_0)/F_0$ are proportional to the concentrations of the chelated iron present when reaction equilibrium is reached, and reflect the chelating efficiency of the iron chelators.

Cell viability assays. CEM T cells were cultured in 96-well plates at 37°C and incubated with iron chelators for the indicated period of time. Cell viability was determined using calcein-AM and trypan blue-based assay. To assess cytotoxicity with calcein-AM, media was removed and the cells were washed with Dulbecco's PBS to remove serum esterase activity that may cause an

increase in fluorescence through the hydrolysis of calcein-AM. Cells were then supplemented with 0.2 µM calcein-AM (Invitrogen) for 10 min at 37°C. A positive control containing 100% dead cells was prepared by treating cells with Triton X-100 [1% (v/v)] that were then incubated with 0.2 µM calcein-AM. Fluorescence was measured using the luminescence spectrometer described above implementing an excitation wavelength of 495 nm and emission filters at 515 nm. To measure cellular viability with trypan blue, the cells were supplemented with 0.2% trypan blue, transferred to a plastic disposable counting chamber and counted on a TC10 Automatic Cell Counter (Bio-Rad).

Luciferase assays. CEM T cells were infected with VSVG-pseudotyped pNL4-3.Luc.R-E-virus prepared as previously described (15) and then cultured at 0.5 x 10^6 cells/mL in 6-well plates at 37°C and 5% CO_2. The cells were collected, washed with PBS and resuspended in 100 µL of PBS. Then, 100 µL of reconstituted luciferase buffer (Luclite Kit, Perkin Elmer) was added to each well and after 10 min incubation, the lysates were transferred into white plates (Perkin Elmer) and luminescence measured using Labsystems Luminoscan RT equipment (Perkin Elmer). PBMCs were purchased from Astarte Biologics (Redmond, WA). Donors were negative for HIV-1 and -2, hepatitis B, hepatitis C and HTLV-1. PBMCs were isolated from peripheral blood by apheresis with additional purification by density gradient centrifugation and cryopreserved until used. PBMCs were activated with phytohemaggultinin (PHA) (0.5 mg/ml) and interleukin (IL)-2 (10 U/ml) for 24 hrs prior to the infection with VSVG-pseudotyped pNL4-3.Luc.R-E- (HIV-1 Luc) virus at approximately 1 ng of p24 per 5 x 10^6 cells. After 48 h, the cells were seeded on 96 well white plates and incubated with the iron chelators for 24 h/37^{o}C.

Then, luciferase buffer was added to each well and luminescence measured using a Labsystems Luminoscan RT, as described above.

To measure luciferase activity in 293T cell, the cells were cultured in 96-well plate and transfected with HIV-1 LTR luciferase vectors and co-transfected with CMV-EGFP to control for the efficiency of transfection. At 48 hours posttransfection, cells were washed three times with PBS and then resuspended in 100 µl of PBS. One hundred microliter of reconstituted luclite buffer (luclite kit, Perkin Elmer) was added to each well. After 10 min of incubation, the cell lysates were transferred to white plates (Perkin Elmer), and luminescence was measured on the Labsystems Luminoscan RT (Perkin Elmer).

Cell cycle analysis of 293T cells treated with iron chelators. Approximately one million cells were fixed in 70% ethanol at -20^{0}C for 2 hours and stained with PI (10 mg/ml) containing RNAse A (1 mg/ml) for 30 minutes. The data were acquired in BD FACS Calibur (BD Biosciences, Jose, California), and analyzed using FlowJo software. Unpaired *t*-test was used to determine statistical significance.

CDK2 and CDK9 phosphorylation assays. 293T cells were treated with iron chelators (1 µM) for 48 hours. Cells were lyzed in whole cell lysis buffer (50 mM Tris-HCl, pH 7.5, 0.3 M NaCl, 1% NP-40, 0.1% SDS) supplemented with protease cocktail (Sigma). CDK2 was immunoprecipitated using anti-CDK2 antibodies. Kinase assay was performed at 30^{o}C for 20 min in the kinase assay buffer containing 2 µg Histone H1 as a substrate, 200 µM ATP and 5 µCi of (γ-^{32}P) ATP. At the end of the incubation, SDS-containing electrophoresis sample buffer was

added to stop the reaction, and protein bands were resolved on 10% SDS-PAGE. Gels were dried and protein bands were visualized by exposing to a Phosphor Imager screen.

Analysis of IKBα, Cyclin A, Cyclin E, and p21 mRNA expression. 293T cells were treated with iron chelators (1 μM) for 48 hours. Total RNA was extracted from cultured 293T cells using TRIzol reagent according to the manufacturer's protocol (Invitrogen). Total RNA (100 ng) was reverse-transcribed to cDNA using Superscript™ RT-PCR kit (Invitrogen, Carlsbad, CA), hexamers and oligo-dT were used as primers. For Real-Time PCR analysis, cDNA was amplified using Roche LightCycler 480 (Roche Diagnostics) and SYBR Green1 Master mix (Roche Diagnostics). PCR was carried with denaturation at 95^{o}C for 10 seconds, annealing at 60^{o}C for 10 seconds, and extension at 72^{o}C for 10 seconds for 45 cycles. For quantification of mRNA levels for p21, CDK2, Cyclin A, Cyclin E and IKBα, β-Actin was used as a house keeping normalization standard. Primer sequences for p21, forward-GCCTTGCAGGAAACTGACTC, reverse- CTTGGCAGCAACTGGATTTT, amplicon Size-183; CDK2 forward- TTTGCTGAGATGGTGACTCG, reverse-CTTCATCCAGGGGAGGTACA, amplicon size 196 bp; Cyclin A, forward-GAAACTGCAGCTCGTAGGAA, reverse-ACTTTCAGAAGCAAGTGTTCCA, amplicon size 150bp; Cyclin E, forward –AGCACTTTCTTGAGCAACACC, reverse-CGCCATATACCGGTCAAAGA, amplicon size 161bp; IKBα, forward-GCCTGGACTCCATGAAAGAC, reverse- GTCTGCTGCAGGTTGTTCTG, amplicon Size-179; β-Actin, forward-AGGCTCAGAGCAAGAGAG, reverse-TACATGGCTGGTGTGTTGA, amplicon size 229. Mean Cp values for p21, CDK2, Cyclin A, cyclin E, IKB, and β-Actin were

251 determined and ΔΔCt method was used to calculate relative expression levels. Unpaired *t*-test
252 was used to determine statistical significance.
253
254 **Separation of large and small P-TEFb complexes by differential salt extraction.** These
255 experiments were performed using the methodology described in our recent publication with
256 slight modifications (13). Briefly, 293T cells in DMEM containing 10% fetal bovine serum were
257 cultured for 48 hours in the absence or presence of 1 μM iron chelators. Cells were washed and
258 resuspended in 500 μl/10^7 cells of Buffer A (10 mM HEPES (pH 7.9), 10 mM KCl, 10 mM
259 $MgCl_2$, 1 mM EDTA, 250 μM sucrose, 1 mM DTT, 0.5% NP-40) supplement with protease
260 inhibitors. The mixture was incubated on ice for 10 min and centrifuged at 1000 x g for 5 min.
261 The supernatant was containing the large complex extract (LC) were collected and stored at -
262 80^{o}C until further analysis. The pellet was resuspended in 500 μl/10^7 cells of Buffer B (20 mM
263 HEPES-KOH (pH 7.9), 450 mM NaCl, 1.5 mM $MgCl_2$, 0.5mM EDTA, 1 mM DTT, and
264 protease inhibitors), incubated on ice for 10 min, and then centrifuged at 10,000 x g for 1 hour.
265 The supernatant containing small complex extract (SC) was collected and stored at -80^{o}C until
266 further analysis (11). The LC and SC were resolved by SDS-PAGE, transferred to a PVDF
267 membrane (Millipore, Allen, TX), and probed with anti-CDK9 and anti-cyclin T1 antibodies.
268
269 **CDK9 kinase assay.** Kinase assay was performed at 30°C for 30 min in a kinase assay buffer
270 (50 mM HEPES-KOH, pH 7.9, 10 mM $MgCl_2$, 6 mM EGTA, 2.5 mM DTT) containing 100 ng
271 of GST-CTD as substrate, 200 μM cold ATP and 5 μCi of (γ-^{32}P) ATP. The kinase reaction was
272 terminated by addition of SDS-PAGE buffer followed by electrophoresis on a 10% SDS-

polyacrylamide gel. The gels were dried and exposed to Phosphor Imager screen to visualize the protein bands.

Immunoprecipitations. For preparation of whole cell lysates, 293T cells were harvested in whole cell lysis buffer (50 mM Tris–HCl buffer, pH 7.5, containing 0.5 M NaCl, 1% NP-40, and 0.1% SDS, containing a cocktail of protease inhibitors) as described above. Immunoprecipitation of CDK9 using anti-CDK9 polyclonal antibody (Santa Cruz) was performed as previously described (13). Briefly, 400 µg of lysate and 800 ng of antibody were incubated for 2 hours at 4^{o}C with 50 µl of 50% protein A/G agarose suspended in 50 mM Tris–HCl, pH 7.5, containing 150 mM NaCl and 1% NP-40 (TNN buffer). The agarose beads were recovered by centrifugation, washed with TNN buffer, resolved on a 10% Tris-Glycine 0.1%SDS gel, transferred to polyvinylidene fluoride (PVDF) membranes and immunoblotted with antibodies against CDK9 or cyclin T1 (Santa Cruz).

Detection and quantification of IKBα, phosphorylated IKBα and NF-κB p65 subunit. 293T cells were cultured at 37^{o}C in the presence or absence of 10 µM iron chelators for 48 hours. For western blot analysis, the cells were lysed in SDS PAGE loading buffer, proteins were resolved by a 10% SDS PAGE and immunoblotted using antibodies against IKBα, IKBα phosphorylated on Ser 32 (IKBα-P) or tubulin as loading control. To analyze NF-κB p65 subunit distribution between the nucleus and cytoplasm, the iron chelators treated cells were lysed in cytoplasm buffer (50 mM Tris–HCl buffer, pH 7.5, containing 0.1% NP-40 and 250 mM sucrose). The cytoplasm was separate from the nuclear material by spinning at 1000xg for 15 min. The cytoplasm and the precipitate nuclear material were separated, lysed in SDS-PAGE loading

buffer, resolved on 10% SDS PAGE and immunoblotted with antibodies against NF-κB p65 subunit or tubulin as loading control. For the immunofluorescence analysis, 293T cells were cultured at 37^{o}C on plastic slides (Nunc, Rochester, NY) in the presence or absence of 10 μM iron chelators for 48 hours. Cells were fixed with 4% formaldehyde, and incubated for 1 hour with primary anti-p65 antibody (1:50, Santa Cruz). Slides were washed with PBS and then incubated for 1 hour with secondary anti-rabbit antibodies conjugated to AlexaFlour 488 (Invitrogen) at a dilution of 1:50. The NF-κB-positive cells were visualized by fluorescence microscope (Olympus IX 510) at 20X magnification.

RT reaction and Quantitative PCR. For quantitative analysis of HIV-1 RNA, total RNA was isolated from various samples including: PBMC lysates, lysates of acute HIV-1 infected (A3R5.7) and chronically HIV-1 infected (J1.1) cell lines. RNA was purified using Trizol Reagent (Invitrogen, Carlsbad, CA) according to the manufacturer's protocol. A total of 0.5μg of RNA from the RNA fraction was treated with 0.25mg/ml DNase I RNase-free (Roche, Mannheim, Germany) for 60 minutes in the presence of 5mM $MgCl_2$, followed by heat inactivation at 65° C for 15 minutes. A 200-250 ng aliquot of total RNA was used to generate cDNA with the GoScript Reverse Transcription System (Promega, Madison, WI) using oligo-dT reverse primer. Subsequent quantitative real-time PCR analysis was performed with 2μl of undiluted and 10^{-1},and 10^{-2} diluted aliquots of RT reaction mixes. The iQ SYBR Green Supermix (Bio-Rad, Hercules, CA) was used with the primers specific for HIV-1 gag gene: Gag1483-F (5'-AAGGGGAAGTGACATAGCAG-3') and Gag1625-R (5'-GCTGGTAGGGCTATACATTCTTAC-3') amplified 143 nt. fragment of HIV-1 gag gene. Serial dilutions of DNA from 8E5 cells (CEM cell line containing a single copy of HIV-1 LAV

provirus per cell) were used as the quantitative standards. To normalize HIV-1 RNA quantifications in the human cells to the target cell DNA, the β-globin gene was quantified by real-time PCR using a set of β-globin-specific primers: BGF1: 5'-CAACCTCAAACAGACACCATGG-3'), BGR1: 5'-TCCACGTTCACCTTGCCC-3' and probe BGX1: 5'-FAM-CTCCTGAGGAGAAGTCTGCCGTTACTGCC-TAMRA-3'. Real-time PCR reactions were carried out at least in triplicate using the PTC-200 Peltier Thermal Cycler with Chromo4 Continuous Fluorescence Detector (both from MJ Research) and Opticon Monitor 2.03 software.

For quantification of HIV-1 DNA, THP-1 cells were infected with HIV-1 Luc and treated with 1 μM iron chelators or 1 μM AZT and further cultured for 48 hours. Total DNA was extracted from $4x10^6$ cells using lysis buffer (10 mM Tris-HCl pH 8, 10 mM EDTA, 5 mM NaCl, 200 μg/ml proteinase K). The cells were lysed for 20-30 min at room temperature and proteinase K was inactivated by heating to 95ºC for 5 min. For the real-time PCR analysis, 100 ng DNA was amplified using Roche Light Cycler 480 (Roche Diagnostics) and SYBR Green1 Master mix (Roche Diagnostics). PCR was carried with initial preincubation for 5 min at 45^0C and then for 3 in at 95^0C followed by 45 cycles of denaturation at 95^oC for 15 sec, annealing and extension at 60^oC for 45 sec, and final extension at 72^oC for 10 sec. Quantification of Early-LTR and Late-LTR was carried using β-globin DNA as a normalization standard. Primer sequences for Early-LTR, forward- GGCTAACTAGGGAACCCACTG, reverse-CTGCTAGAGATTTTCCACACTGAC; Late-LTR forward- TGTGTGCCCGTCTGTTGTGT, reverse- GAGTCCTGCGTCGAGAGATC, Globin, forward-CAACCTCAAACAGACACCATGG, reverse- TCCACGTTCACCTTGCCC (see (30) for

primer information). Mean Cp values for Early-LTR, Late-LTR and β-globin were determined and ΔΔCt method was used to calculate relative expression levels. Unpaired *t*-test was used to test statistical significance.

Results

Chemical structures of PPY-based iron chelators. In a previous study, we screened a number of di-2-pyridylketone thiosemicarbazone (DpT) and 2-benzoylpyridine thiosemicarbazone (BpT)-based tridentate iron chelators for HIV-1 inhibition and identified Dp44eT, Bp4aT and Bp4eT chelators as most efficient and suitable for further modifications (15) (Fig.1A). All of these chelators were shown to be toxic in vivo (31). Since the diarylketone and thiosemicarbozone moieties are likely to adopt a planar conformation that could potentially increase their ability to intercalate DNA, we substituted benzyl group for the phenyl group. The benzyl analogs, PPYaT and PPYeT were synthesized (see Materials and Methods) along with the non-chelating PPY compound that served as negative treatment control. The chemical structures of PPY-based iron chelators are shown in Figure 1 (B-D).The PPY-based iron chelators was analyzed by high resolution mass spectrometry for purity (Fig. 1, panels E-G) and also by NMR (not shown). Both PPYeT and PPYaT were found to contain PPY and their purity was 85% and 90% respectively (Fig. 1, F and G).

PPYaT and PPYeT efficiently chelate cellular iron. The ability of PPY-based compounds to chelate iron was tested in the promonocytic THP-1 cells as previously described (29) and because of these cells capability to handle iron. THP-1 cells were treated with non-fluorescent cell-permeable calcein-AM, which, after being transported into the cells, is converted to calcein,

a weak iron-binding fluorescent compound, whose fluorescence is quenched upon binding to iron. THP-1 cells were pretreated with FeS and then loaded with calcein-AM. After washing the excess of calcein-AM the cells were treated with non-chelating PPY compound, and iron chelators, PPYeT, PPYaT and, as positive control, cylaldehyde isonicotinyl hydrazone (SIH) (32). As shown in Fig. 2A, the gain of fractional fluorescence $(F-F_0)/F_0$, which is directly proportional to the amount of chelatable iron, was similar for PPYeT and SIH but it was slightly less for PPYaT. Non-chelating PPY compound had no effect on the gain of fractional fluorescence. These results indicate that both PPYeT and PPYaT were able to chelate iron in cultured cells to extent observed with SIH. Next, we analyzed the effect of PPY-based iron chelators on the levels of transferrin receptor (TFR) mRNA which contains iron responsive elements (IREs) in the 3'UTR which, when bound to iron responsive protein (IRP), stabilize RNA (33). Thus the level of mRNA reflects the amount of cellular iron that assembles into the iron-sulfur cluster of IRP, prevents their binding to IREs and destabilizes TFR mRNA (33). Real-time PCR analysis revealed a significant increase in TFR mRNA levels in cells treated with PPYaT and PPYeT but not PPY or DMSO vehicle control (Fig.2B), further indicating that PPY-based iron chelators reduce the intracellular iron content.

Treatment with PPYaT or PPYeT leads to the arrest of cells in G1/S phase. Iron chelators are known to arrest the cell cycle (34, 35). Therefore, we examined the effects of PPY-based iron chelators on the cell cycle progression of THP-1, CEM or 293T cells (Fig.2, C-E). The cells treated with DMSO or control PPY compound showed about 50-55% of the cells in G1 cell cycle (Fig.2, C-E). THP-1 and CEM cells showed about 35% G2/M phase and 10% of S phase whereas 293T cells showed about 20% G2/M phase and 20% C phase (Fig.2, C-E). The different

388 effects on different cell types are likely to reflect different growth properties of these cells.
389 Treatment with PPYeT or PPYaT iron chelators, resulted in a sharp decrease of the cell number
390 in G2/M phase and increased G1 phase accumulation (Fig.2, C-E).
391
392 **PPYaT and PPYeT inhibit one round HIV-1 infection in cultured T cells and PBMC.** The
393 effect of PPY-based iron chelators on one-round HIV-1 infection was analyzed in CEM T cells
394 infected with VSV-G pseudotyped HIV-1 pNL4-3 virus expressing luciferase in place of *nef*
395 (HIV-1 Luc) (36). Luciferase activity was measured as an indicator of HIV-1 gene expression.
396 HIV-1 expression was inhibited by PPYaT or PPYeT chelators, but not by the control compound
397 PPY, or DMSO which was used as normalization point, at nanomolar concentrations (EC_{50}=14
398 nM) (Fig.2A). The PPY-based iron chelators showed no toxicity below 10 μM concentration in
399 CEM T cell incubated with the chelators for 24 hours at 37^{o}C (Fig.2B). We also analyzed the
400 effects of PPYaT and PPYeT iron chelators on one-round of HIV-1 infection in peripheral blood
401 mononuclear cells (PBMC). The cells were activated with phytohemagglutinin (PHA) and IL-2
402 (described in Materials and Methods) and then infected with HIV-1 Luc. After 48 hours, the cells
403 were treated for 24 hours with PPY-based iron chelators and PPY as control, and then analyzed
404 for luciferase activity. As shown in Fig.3C, PPYaT and PPYeT, but not PPY, markedly inhibited
405 HIV-1 replication at EC_{50}~1 μM. Cytotoxic effects of iron chelators in PBMC, determined by
406 trypan blue exclusion test using automatic cell counter showed no significant cell death up to 100
407 μM for PPYaT or control PPY treated cells (Fig. 3D). In contrast, PPYeT showed about 50%
408 reduction of viability at 96 μM concentration. Thus, taken together, these results indicate that
409 PPY-based iron chelators markedly inhibited HIV-1 infection of T cells and PBMCs. PPYaT
410 showed less toxicity than PPYeT.

411 **Effect of PPY-based iron chelators on HIV-1 transcription in acutely and chronically**
412 **infected T cells and PBMCs.** We analyzed the effect of the least toxic PPYaT iron chelator on
413 HIV-1 in A2R5.7 T cells acutely infected with HIV-1 subtype B or subtype C (Fig.4, A and B).
414 Analysis of unspliced viral RNA showed about 3-fold decrease of HIV-1 expression even at the
415 lowest 0.3 μM concentration (Fig.4A). In contrast, acute infection with HIV-1 subtype C showed
416 no effect of PPYaT at 0.3 μM concentration and about 2 fold inhibition at 3 μM concentration
417 (Fig.4B). We next investigated the effect of iron chelators on HIV-1 expression in chronically
418 infected J1.1 T cells (Fig. 4C). The cells were pretreated with cART cocktail for 7 days to avoid
419 HIV-1 replication and reinfection. Treatment with iron chelators reduced HIV-1 RNA production
420 for up to 3-fold by PPYeT at 10 μM concentration (Fig.4C). Finally we tested the effect of iron
421 chelators on HIV-1 transcription in acutely infected PBMCs. The PBMCs that were obtained
422 from three different donors were infected with dual-tropic HIV-1 strain 89.6 and then treated
423 with iron chelators for 48 h. Analysis of HIV-1 unspliced RNA showed significant , 2-3 fold
424 reduction of HIV-1 expression (Fig.4D). Taken together, these results indicate that iron chelators
425 strongly inhibit HIV-1 transcription of HIV-1 subtype B in chronically and acutely infected
426 primary and culture T cells. The effect of iron chelators on subtype C was less pronounced
427 suggesting that iron chelators may not be suitable to inhibit all HIV-1 subtypes and indicating
428 subtype specificity for iron responsiveness.
429
430 **Treatment with PPYaT or PPYeT leads to the induction of IKBα expression and**
431 **redistribution of NF-κB p65 subunit.** Because iron chelators showed to accumulate cells at G1
432 phase of the cell cycle, we examined the effects of PPY-based iron chelators on the expression
433 levels of CDK2-associated cyclins and CDK9-dependent genes, HLA and IKBα. We used 18S

RNA as normalization housekeeping control as it was shown to be the most reliable house keeping control among several tested that included ACTB and GAPDH (37). Treatment with PPYaT or PPYeT induced expression of cyclin A and cyclin E (Fig.5A). The slight increase in the CDK2 expression was not statistically significant. There was no effect on HLA expression while, IKBα expression showed significant, more than 10-fold increase of IKBα protein level (Fig.5B). No significant increase in IKBα phosphorylation on Ser32 residue was detected (Fig.5B) suggesting that IKBα was not undergoing degradation and that NF-κB levels might be modulated. We observed increased expression of p21 but no increase in its protein levels (data not shown) as previously reported by Des Richardson and his colleagues (38). To determine whether the iron chelators affected the expression and cytoplasmic localization of NK-kB, we analyzed the level of NF-κB expression and its distribution between the nucleus and the cytoplasm. We found significantly higher levels of NF-κB localized in the cytoplasm in PPYeT or PPYaT-treated cells comparing to the PPY control (Fig.5C). Analysis of NF-κB p65 expression in cytoplasm and nucleus by immunoblotting showed localization of p65 in the cytoplasm in the chelator's treated cells in comparison to the cells treated with PPY control (Fig.5D). Taken together, these results indicate that iron chelators have strong effect on NF-κB.

Iron chelators inhibit CDK2 activity and reduce the formation of large P-TEFb complex. . While we could not detect changes in the p21 expression levels, our previous studies suggest that CDK2 activity is reduced by chelators-treated cells (15, 16). To determine whether the PPY-based iron chelators inhibit CDK2 activity, 293T cells were cultured for 48 hours at 37^{o}C in the presence or absence of the iron chelators using PPY compound as a control. CDK2 was immunoprecipitated from cell lysates by anti-CDK2 antibodies and assayed using histone H1 as

457 a substrate (see details in Materials and Methods). Treatment of cells with iron chelators reduced
458 the CDK2 activity by about 3-fold (Fig.6A). To further examine the effect of PPY-based iron
459 chelators on CDK9 activity, Flag-tagged-CDK9 and cyclin T1 were expressed in 293T cells and
460 treated with the iron chelators, CDK9 was immunoprecipitated from cell lysates with anti-Flag
461 antibodies and its activity was assayed with Rb-CTF peptide as a substrate. The CDK9 activity
462 was increased in PPYeT-treated cells with a slightly decrease in PPYaT treated cells (Fig.6B).
463 While an increase in CDK9 activity was unexpected, it reflects the increase of small molecular
464 weight CDK9/cyclin T1 which disfavors HIV-1 transcription that uses large molecular weight P-
465 TEFb as a source of CDK9/cyclin T1. Thus we investigated the effect of iron chelators on large
466 and small P-TEFb complexes.
467
468 To determine the effects of iron chelators on CDK9/cyclin T1, we used salt extraction procedure
469 that we previously utilized to determine the effect of CDK2 knock down on P-TEFb (13). CDK9
470 and cyclin T1 were expressed in 293T and then the large and small P-TEFb complexes were
471 extracted using low and high salt lysis buffers. As shown in Fig. 7 (A-C), the large P-TEFb
472 complex isolated from the iron-chelators-treated cells contained substantially less amounts of
473 both CDK9 and cyclin T1. In contrast, the level of cyclin T1 was significantly increased in the
474 small complex (Fig.7A and C). These results suggest that CDK9/cyclin T1 associate less
475 efficiently with the large P-TEFb complex in the iron chelators treated cells. This results is
476 consistent with our previous findings that CDK2 knock down decreases the amount of large P-
477 TEFb complex (13).
478

Iron chelators reduce HIV-1 mRNA expression but do not inhibit HIV-1 reverse transcription. To further elucidate the mechanism of HIV-1 inhibition by PPY-based iron chelators, we analyzed HIV-1 mRNA expression in CEM T cells infected with HIV-1 Luc virus. Expression of Gag and Env-coding mRNAs was significantly reduced by treatment PPYeT or PPYaT in comparison to DMSO or PPY-treated controls (Fig.8A). We noticed that DMSO treatment induced Gag and Env expression (Fig.8A) in accord with previous observation (39). We also analyzed whether iron chelators have an effect on HIV-1 reverse transcription. We analyzed early reverse transcription (RT) by quantifying HIV-1 DNA for Early LTR (30). The established HIV-1 inhibitor, azidothymidine (AZT) showed statistically significant effect on HIV-1 LTR expression whereas iron chelators showed no effect (Fig.8B). Thus, iron chelators had no inhibitory effect on HIV-1 RT while reducing HIV-1 transcription as evidenced by the reduction of HIV-1 Gag and Env gene expression.

Inhibition of basal HIV-1 transcription by PPY-based iron chelators. To further investigate the effect of iron chelators on HIV-1 transcription, we examined their effect in 293T cells transfected with vectors expressing luciferase under control of various HIV-1 LTR mutants (see Material and Methods for details). Treatment with PPYaT or PPYeT iron chelators had moderate (less than 2-fold) but statistically significant inhibitory effect on WT HIV-1 LTR-driven transcription (Fig.8C). We also observed similar effect on HIV-1 LTR with deletions of NF-κB or Sp1 sites (Fig. 8, D and E). HIV-1 basal transcription is regulated by Sp1 and NF-κB (23, 25) in conjunction with NF-κB that cooperates with Tat in Tat-activated HIV-1 transcription (2). Thus, the relatively moderate effect of iron chelators on basal HIV-1 transcription could be

amplified because of the inability of HIV-1 Tat to engage Sp1 or NF-κB for the induction of HIV-1 transcription.

Discussion

Our results presented here demonstrate that the synthetically modified novel PPY-based iron chelators with benzyl group substituted for the phenyl group are effective in chelating intracellular iron and inhibiting HIV-1 transcription. The PPY-based compounds chelated cellular labile iron with the efficiency similar to SIH. They also promoted synthesis of transferrin receptor mRNA, suggesting that cellular iron was substantially reduced. The PPY-based iron chelators are similar to the previously studied HIV-1 inhibitory benzoylpyridine thiosemicarbazone compounds that also chelate cellular labile iron similar to SIH (40). Only one aromatic ring was shown to be required to coordinate the binding of iron (31). Therefore, the benzyl moiety of PPY-based compound can be further utilized for optimization of other properties such as adjustment of ADME-Tox profile. We observed good therapeutic window for for PPYaT chelator in CEM T cells and PBMCs under the concentration range tested (see Fig.3). PPYeT, on the other hand, showed some toxicity both in CEM T cells and PBMCs and less favorable therapeutic window , which was consistent with its higher potency to chelate iron.

Previously, administration of Dp44mT in mice showed little alteration in hematological and biochemical indices (0.4–0.75 mg/kg/day), but induced anti-tumor activity (5). The BpT-based iron chelators showed greater anti-neoplastic activity than their DpT homologs *in vitro* (6). Recently, Dp44mT showed a significant methemoglbin (metHb) formation in intact red blood cells and in mice (31). A modified analog, di-2-pyridylketone-4-cyclohexyl-4-methyl-3-thiosemicarbazone did not generate production of metHb and thus was proposed to be suitable

for further optimization (31). Also, BpT was shown to induce metHb whereas its analog, lipophylic t-BuBpT chelator was less potent inducer of metHb (41). Thus, PPY-based iron chelators may also potentially induce MetHb formation and further optimization may be needed to alleviate this effect. Benzyl moiety of PPY-based compound can be used to further optimization as mentioned above.

In early studies, iron chelators were shown to inhibit cell cycle progression which coincided with the inhibition of CDK2 enzymatic activity (34, 35). Iron chelators were shown to increase p21 mRNA and protein expression (42). The expression of p21 was also shown to be increased by HIF-1α which displaced c-myc on the p21 promoter (43). We previously demonstrated that iron chelators, 311, ICL670, Bp4eT and Dp4eT inhibit the activity of CDK2 (15, 16). Here, we show that PPY-based iron chelators inhibit cell cycle progression of promonocytic THP-1 cells, CEM T cells and epithelial 293T cells. We were not able to detect increased p21 protein expression. However, reduced p21 expression can also be inhibitory for CDK2/cyclin E which requires low levels of p21 that is used as a scaffold for the assembly of CDK2/cyclin E complex (44). In agreement with our previous studies, CDK2 activity was significantly reduced. Whether the decreased CDK2 activity might be mediated by a deregulation of p21 remains to be determined. The decrease in the cell cycle progression coincided with the increased expression of cyclin A and cyclin E, whereas the expression of CDK2 was unchanged. CDK9 activity was increased in the PPYeT-treated cells likely due to the shift of CDK9/cyclin T1 from the large to the small p-TEFb complex, which was more prominent in the PPYeT-treated cells. We observed similar effect in CDK2 knock-down cells (not shown). We recently showed that CDK2 phosphorylates CDK9 Ser90, and that lack of this phosphorylation disrupted the formation of the large P-TEFb

548 complex (13). Thus, the reduction of the large P-TEFb complex is likely to be due to the
549 reduction of CDK2 activity and CDK9 phosphorylation.
550
551 We observed the strong inhibitory effect of PPYaT on cultured T cells infected with HIV-1
552 subtype B, but less so by HIV subtype C. Previously, subtype C was shown to exhibit slower
553 replication due to different enzymatic activity of its reverse transcriptase (45). Thus, iron
554 chelators may not be efficient against all HIV subtypes and whether they have effect on other
555 HIV subtypes remain to be determined. We also observed the inhibition of HIV-1 gene
556 expression in latently infected T cells and also inhibition of acute HIV-1 infection of primary
557 PBMCs by HIV-1 subtype B. These results indicate that PPY-based iron chelators are likely to
558 inhibit HIV-1 transcription. The EC_{50}s varied depending on the cell types used. The lowest
559 EC50s were observed in CEM T cells in accord to our previous study of HIV-1 inhibition by
560 BpT and DpT iron chelators that showed low nanomolar EC_{50}s in CEM T cells (15). These low
561 EC_{50}s are likely to reflect unusual sensitivity of this leukemia cell line to iron chelators which is
562 reflected in relatively high toxicity of the chelators in this cell line. In PBMCs, the chelators
563 showed much higher EC_{50} for HIV-1 inhibition but also much lower toxicity. Ultimately, in vivo
564 testing of the chelators in an animal model, such as HIV-1 infected humanized mice will
565 determine their in vivo toxicity and efficacy for HIV-1 inhibition.
566
567 CDK9/cyclin T1 induces expression of IL-8 and Gro-β (46) and represses expression of MHC
568 class II genes such as HLA-DRA (47). We have previously shown that hypoxia decreases the
569 expression of IKBα but not Gro-β or HLA-DRA (48). Data presented in this report suggest that
570 inhibition of CDK9-depedent genes by PPY-based iron chelators could lead to the over

571 expression of IKBα but have no effect on HLA expression. To our knowledge, this is the first
572 demonstration of IKBα expression linking to the reduction of cellular iron. HIV-1 basal
573 transcription is largely regulated by the Sp1 transcription factor (23), whereas in Tat activated
574 transcription, NF-κB plays an important regulatory role by acting in concert with Tat and
575 CDK9/cyclin T1 (2). NF-κB might recruit CDK9/cyclin T1 to HIV-1 LTR in a cooperative
576 manner (20, 21), in part, because of the interaction of Tat with the p65 subunit of NF-κB through
577 NFBP protein (22). In the absence of TAR RNA, Cyclin T1 can be recruited to the LTR by Sp1
578 (24). NF-κB regulates expression of a large number of genes that are critical induction of
579 apoptosis, viral replication, tumorigenesis, inflammation, and various autoimmune diseases (49).
580 NF-κB is composed of homo- and heterodimers of five members of the Rel family including NF-
581 κB 1(p50), NF-κB 2 (p52), Rel A, Rel B, and c-Rel (Rel) (49). Inactive NF-κB is sequestered in
582 the cytoplasm, bound by members of the IKB family of inhibitory proteins, which include IKBα,
583 IKBβ, IKBγ, and IKBδ (49). IKBs phosphorylation by IKKs leads to their ubiquitination and
584 subsequent degradation that exposes the nuclear localization signal of NF-κB and help to
585 translocate it to the nucleus (50). Our analysis showed that increased expression of IKBα
586 coincides with the accumulation of NF-κB in cytoplasm and reduction of NF-κB in the nucleus.
587 Thus, in the PPY-based iron chelators treated cells, NF-κB is unavailability for HIV-1
588 transcription activation contributing to the inhibition of HIV-1. Similarly, IKBα expression was
589 increased in stable CDK2 knockdown cell lines (data not shown) suggesting that CDK2
590 negatively regulates its expression.
591
592 In addition to the inhibition of HIV-1 transcription, iron depletion may affect other steps in HIV-
593 1 replication (reviewed in (51)). During viral entry, HIV-1 replication is dependent on the

activity of host cell ribonucleotide reductase (RNR) that contains non heme iron, which is important for its enzymatic activity (52). Recently, expression of p21 was shown to down-regulate the expression of the RNR2 subunit that decreased intracellular deoxyribonucleotide (dNTP) pool and impaired HIV-1 and SIV reverse transcription (53). Expression of p21 inhibited RNR2 transcription by repressing E2F1 transcription factor which activates RNR2 transcription (53). While we have not analyzed the dNTP pools, we have not seen a reduction in the HIV-1 reverse transcription and, therefore, PPY-based iron chelators are not likely to affect RNR2. Export of unspliced HIV-1 mRNA requires HIV-1 Rev protein and host elongation factor 5A (eIF5α) which contains *N*-epsilon-4-amino-2-hydroxybutyl-lysine (hypusine) produced by deoxyhypusine hydroxylase (DOHH), an iron-containing enzyme (54). Topical fungicide, cyclopirox, and the iron chelator, deferiprone, were shown to inhibit HIV-1 gene expression interfering with the hydroxylation step in the hypusine modification of eIF5α (55). More recently, ciclopirox and deferiprone were shown to induce apoptosis though mitochondrial membrane depolarization in HIV-infected T cells thus promoting selective elimination of HIV-1 infected cells in long-term culture (56). Whether PPY-based iron chelators can specifically eliminate HIV-1 infected cells remain to be determined.

Finally, it must be noted that the very different mechanism of action of these chelators compared with other established antiviral therapies may present an advantage for the future use of iron chelators. They could be potentially useful for treatment of resistant viral infection which is a major problem for the existing antiretroviral drugs. Many common chemotherapeutic drugs currently in clinical use, such as doxorubicin, display marked cytotoxicity profiles *in vitro* (57), but are well tolerated at appropriate doses *in vivo* and have led to vast improvements in cancer

617 treatment. As discussed above Thus PPY-based iron chelators can be further modified to reduce
618 their potential pharmacological toxicity in vivo and improve their potential future use as anti-
619 HIV-1 therapeutic agents.
620
621 Taken together, low EC_{50} of PPY-based iron chelators and their good therapeutic window
622 indicate their application in future potentially useful anti-retroviral therapeutics. Hence, these
623 compounds may pave a way to treat subjects infected with HIV-1 with high iron load, a
624 condition shown to be related to the progression of HIV-1 infection (58).
625

626 **Acknowledgements**

627 This work was supported by NIH Research Grants (1SC1GM082325, 1P50HL118006-01,
628 1R01HL125005-01, U19AI109664-01 and 5G12MD007597), and District of Columbia
629 Developmental Center for AIDS Research grant (P30AI087714). The authors would like to
630 thank NIH AIDS Research and Reference Reagent Program for pHEF-VSVG expression vector
631 (courtesy of Dr. Lung-Ji Chang) and pNL4-3.Luc.R^-E^- (courtesy of Dr. Nathaniel Landau).
632

633 **Competing interests**

634 No financial competing interests are declared.
635

636 **Authors' contributions**: NK conducted the research, analyzed results, and wrote the
637 manuscript. SI conducted experiment with chronically and acutely infected cultured and primary
638 cells and participated in the manuscript preparation. DB, XN and MX conducted the research and
639 analyzed results. DK and KG designed and synthesized iron chelator and contributed to the

preparation of the manuscript. XL analyzed the purity of iron chelators using LC-MS. SD and FK participated in the study design and writing of the manuscript. SN takes primary responsibility for the paper. SN conducted design and performed some experiments, analyzed results, and drafted the manuscript. The findings and conclusions in this paper have not been formally disseminated by the Food and Drug Administration and should not be construed to represent any Agency determination or policy.

References

1. **Lu H, Li Z, Xue Y, Zhou Q.** 2013. Viral-Host Interactions That Control HIV-1 Transcriptional Elongation. Chem Rev.
2. **West MJ, Lowe AD, Karn J.** 2001. Activation of human immunodeficiency virus transcription in T cells revisited: NF-kappaB p65 stimulates transcriptional elongation. J Virol **75:**8524-8537.
3. **He N, Jahchan NS, Hong E, Li Q, Bayfield MA, Maraia RJ, Luo K, Zhou Q.** 2008. A La-related protein modulates 7SK snRNP integrity to suppress P-TEFb-dependent transcriptional elongation and tumorigenesis. Mol Cell **29:**588-599.
4. **Krueger BJ, Jeronimo C, Roy BB, Bouchard A, Barrandon C, Byers SA, Searcey CE, Cooper JJ, Bensaude O, Cohen EA, Coulombe B, Price DH.** 2008. LARP7 is a stable component of the 7SK snRNP while P-TEFb, HEXIM1 and hnRNP A1 are reversibly associated. Nucleic Acids Res **36:**2219-2229.
5. **Markert A, Grimm M, Martinez J, Wiesner J, Meyerhans A, Meyuhas O, Sickmann A, Fischer U.** 2008. The La-related protein LARP7 is a component of the 7SK ribonucleoprotein and affects transcription of cellular and viral polymerase II genes. EMBO Rep **9:**569-575.
6. **Barboric M, Lenasi T, Chen H, Johansen EB, Guo S, Peterlin BM.** 2009. 7SK snRNP/P-TEFb couples transcription elongation with alternative splicing and is essential for vertebrate development. Proc Natl Acad Sci U S A **106:**7798-7803.
7. **Jeronimo C, Forget D, Bouchard A, Li Q, Chua G, Poitras C, Therien C, Bergeron D, Bourassa S, Greenblatt J, Chabot B, Poirier GG, Hughes TR, Blanchette M, Price DH, Coulombe B.** 2007. Systematic analysis of the protein interaction network for the human transcription machinery reveals the identity of the 7SK capping enzyme. Mol Cell **27:**262-274.
8. **Sobhian B, Laguette N, Yatim A, Nakamura M, Levy Y, Kiernan R, Benkirane M.** 2010. HIV-1 Tat assembles a multifunctional transcription elongation complex and stably associates with the 7SK snRNP. Mol Cell **38:**439-451.
9. **He N, Liu M, Hsu J, Xue Y, Chou S, Burlingame A, Krogan NJ, Alber T, Zhou Q.** 2010. HIV-1 Tat and host AFF4 recruit two transcription elongation factors into a

bifunctional complex for coordinated activation of HIV-1 transcription. Mol Cell **38:**428-438.

10. **Yang Z, Zhu Q, Luo K, Zhou Q.** 2001. The 7SK small nuclear RNA inhibits the CDK9/cyclin T1 kinase to control transcription. Nature **414:**317-322.
11. **Nguyen VT, Kiss T, Michels AA, Bensaude O.** 2001. 7SK small nuclear RNA binds to and inhibits the activity of CDK9/cyclin T complexes. Nature **414:**322-325.
12. **Sedore SC, Byers SA, Biglione S, Price JP, Maury WJ, Price DH.** 2007. Manipulation of P-TEFb control machinery by HIV: recruitment of P-TEFb from the large form by Tat and binding of HEXIM1 to TAR. Nucleic Acids Res **35:**4347-4358.
13. **Breuer D, Kotelkin A, Ammosova T, Kumari N, Ivanov A, Ilatovskiy AV, Beullens M, Roane PR, Bollen M, Petukhov MG, Kashanchi F, Nekhai S.** 2012. CDK2 regulates HIV-1 transcription by phosphorylation of CDK9 on serine 90. Retrovirology **9:**94.
14. **Jerebtsova M, Kumari N, Xu M, de Melo GB, Niu X, Jeang KT, Nekhai S.** 2012. HIV-1 Resistant CDK2-Knockdown Macrophage-Like Cells Generated from 293T Cell-Derived Human Induced Pluripotent Stem Cells. Biology (Basel) **1:**175-195.
15. **Debebe Z, Ammosova T, Breuer D, Lovejoy DB, Kalinowski DS, Kumar K, Jerebtsova M, Ray P, Kashanchi F, Gordeuk VR, Richardson DR, Nekhai S.** 2011. Iron chelators of the di-2-pyridylketone thiosemicarbazone and 2-benzoylpyridine thiosemicarbazone series inhibit HIV-1 transcription: identification of novel cellular targets--iron, cyclin-dependent kinase (CDK) 2, and CDK9. Mol Pharmacol **79:**185-196.
16. **Debebe Z, Ammosova T, Jerebtsova M, Kurantsin-Mills J, Niu X, Charles S, Richardson DR, Ray PE, Gordeuk VR, Nekhai S.** 2007. Iron chelators ICL670 and 311 inhibit HIV-1 transcription. Virology **367:**324-333.
17. **Chen H, Li C, Huang J, Cung T, Seiss K, Beamon J, Carrington MF, Porter LC, Burke PS, Yang Y, Ryan BJ, Liu R, Weiss RH, Pereyra F, Cress WD, Brass AL, Rosenberg ES, Walker BD, Yu XG, Lichterfeld M.** 2011. CD4+ T cells from elite controllers resist HIV-1 infection by selective upregulation of p21. J Clin Invest **121:**1549-1560.
18. **Ammosova T, Berro R, Jerebtsova M, Jackson A, Charles S, Klase Z, Southerland W, Gordeuk VR, Kashanchi F, Nekhai S.** 2006. Phosphorylation of HIV-1 Tat by CDK2 in HIV-1 transcription. Retrovirology **3:**78.
19. **Adesina SK, Holly A, Kramer-Marek G, Capala J, Akala EO.** 2014. Polylactide-Based Paclitaxel-Loaded Nanoparticles Fabricated by Dispersion Polymerization: Characterization, Evaluation in Cancer Cell Lines, and Preliminary Biodistribution Studies. J Pharm Sci.
20. **Barboric M, Nissen RM, Kanazawa S, Jabrane-Ferrat N, Peterlin BM.** 2001. NF-kappaB binds P-TEFb to stimulate transcriptional elongation by RNA polymerase II. Mol Cell **8:**327-337.
21. **Deng L, de la Fuente C, Fu P, Wang L, Donnelly R, Wade JD, Lambert P, Li H, Lee CG, Kashanchi F.** 2000. Acetylation of HIV-1 Tat by CBP/P300 increases transcription of integrated HIV-1 genome and enhances binding to core histones. Virology **277:**278-295.
22. **Sweet T, Sawaya BE, Khalili K, Amini S.** 2005. Interplay between NFBP and NF-kappaB modulates tat activation of the LTR. J Cell Physiol **204:**375-380.

23. **Jochmann R, Thurau M, Jung S, Hofmann C, Naschberger E, Kremmer E, Harrer T, Miller M, Schaft N, Sturzl M.** 2009. O-linked N-acetylglucosaminylation of Sp1 inhibits the human immunodeficiency virus type 1 promoter. J Virol **83:**3704-3718.
24. **Yedavalli VS, Benkirane M, Jeang KT.** 2003. Tat and trans-activation-responsive (TAR) RNA-independent induction of HIV-1 long terminal repeat by human and murine cyclin T1 requires Sp1. J Biol Chem **278:**6404-6410.
25. **Chun RF, Semmes OJ, Neuveut C, Jeang KT.** 1998. Modulation of Sp1 phosphorylation by human immunodeficiency virus type 1 Tat. J Virol **72:**2615-2629.
26. **Westervelt P, Trowbridge DB, Epstein LG, Blumberg BM, Li Y, Hahn BH, Shaw GM, Price RW, Ratner L.** 1992. Macrophage tropism determinants of human immunodeficiency virus type 1 in vivo. J Virol **66:**2577-2582.
27. **Grisson RD, Chenine AL, Yeh LY, He J, Wood C, Bhat GJ, Xu W, Kankasa C, Ruprecht RM.** 2004. Infectious molecular clone of a recently transmitted pediatric human immunodeficiency virus clade C isolate from Africa: evidence of intraclade recombination. J Virol **78:**14066-14069.
28. **Gomez-Gonzalo M, Carretero M, Rullas J, Lara-Pezzi E, Aramburu J, Berkhout B, Alcami J, Lopez-Cabrera M.** 2001. The hepatitis B virus X protein induces HIV-1 replication and transcription in synergy with T-cell activation signals: functional roles of NF-kappaB/NF-AT and SP1-binding sites in the HIV-1 long terminal repeat promoter. J Biol Chem **276:**35435-35443.
29. **Epsztejn S, Kakhlon O, Glickstein H, Breuer W, Cabantchik I.** 1997. Fluorescence analysis of the labile iron pool of mammalian cells. Anal Biochem **248:**31-40.
30. **Vermeire J, Naessens E, Vanderstraeten H, Landi A, Iannucci V, Van Nuffel A, Taghon T, Pizzato M, Verhasselt B.** 2012. Quantification of reverse transcriptase activity by real-time PCR as a fast and accurate method for titration of HIV, lenti- and retroviral vectors. PLoS One **7:**e50859.
31. **Quach P, Gutierrez E, Basha MT, Kalinowski DS, Sharpe PC, Lovejoy DB, Bernhardt PV, Jansson PJ, Richardson DR.** 2012. Methemoglobin formation by triapine, di-2-pyridylketone-4,4-dimethyl-3-thiosemicarbazone (Dp44mT), and other anticancer thiosemicarbazones: identification of novel thiosemicarbazones and therapeutics that prevent this effect. Mol Pharmacol **82:**105-114.
32. **Simunek T, Boer C, Bouwman RA, Vlasblom R, Versteilen AM, Sterba M, Gersl V, Hrdina R, Ponka P, de Lange JJ, Paulus WJ, Musters RJ.** 2005. SIH--a novel lipophilic iron chelator--protects H9c2 cardiomyoblasts from oxidative stress-induced mitochondrial injury and cell death. J Mol Cell Cardiol **39:**345-354.
33. **Rouault TA.** 2006. The role of iron regulatory proteins in mammalian iron homeostasis and disease. Nat Chem Biol **2:**406-414.
34. **Lucas JJ, Szepesi A, Domenico J, Takase K, Tordai A, Terada N, Gelfand EW.** 1995. Effects of iron-depletion on cell cycle progression in normal human T lymphocytes: selective inhibition of the appearance of the cyclin A-associated component of the p33cdk2 kinase. Blood **86:**2268-2280.
35. **Pahl PM, Yan XD, Hodges YK, Rosenthal EA, Horwitz MA, Horwitz LD.** 2000. An exochelin of Mycobacterium tuberculosis reversibly arrests growth of human vascular smooth muscle cells in vitro. J Biol Chem **275:**17821-17826.

36. **He J, Landau NR.** 1995. Use of a novel human immunodeficiency virus type 1 reporter virus expressing human placental alkaline phosphatase to detect an alternative viral receptor. J Virol **69:**4587-4592.
37. **Kuchipudi SV, Tellabati M, Nelli RK, White GA, Perez BB, Sebastian S, Slomka MJ, Brookes SM, Brown IH, Dunham SP, Chang KC.** 2012. 18S rRNA is a reliable normalisation gene for real time PCR based on influenza virus infected cells. Virol J **9:**230.
38. **Le NT, Richardson DR.** 2003. Potent iron chelators increase the mRNA levels of the universal cyclin-dependent kinase inhibitor p21(CIP1/WAF1), but paradoxically inhibit its translation: a potential mechanism of cell cycle dysregulation. Carcinogenesis **24:**1045-1058.
39. **Klebanoff SJ, Mehlin C, Headley CM.** 1997. Activation of the HIV type 1 long terminal repeat and viral replication by dimethylsulfoxide and related solvents. AIDS Res Hum Retroviruses **13:**1221-1227.
40. **Debebe Z, Nekhai S, Ashenafi M, Lovejoy DB, Kalinowski DS, Gordeuk VR, Byrnes WM, Richardson DR, Karla PK.** 2012. Development of a sensitive HPLC method to measure in vitro permeability of E- and Z-isomeric forms of thiosemicarbazones in Caco-2 monolayers. J Chromatogr B Analyt Technol Biomed Life Sci **906:**25-32.
41. **Stefani C, Jansson PJ, Gutierrez E, Bernhardt PV, Richardson DR, Kalinowski DS.** 2013. Alkyl substituted 2'-benzoylpyridine thiosemicarbazone chelators with potent and selective anti-neoplastic activity: novel ligands that limit methemoglobin formation. J Med Chem **56:**357-370.
42. **Moon SK, Jung SY, Choi YH, Lee YC, Patterson C, Kim CH.** 2004. PDTC, metal chelating compound, induces G1 phase cell cycle arrest in vascular smooth muscle cells through inducing p21Cip1 expression: involvement of p38 mitogen activated protein kinase. J Cell Physiol **198:**310-323.
43. **Koshiji M, Kageyama Y, Pete EA, Horikawa I, Barrett JC, Huang LE.** 2004. HIF-1alpha induces cell cycle arrest by functionally counteracting Myc. EMBO J **23:**1949-1956.
44. **Gartel AL.** 2006. Inducer and inhibitor: "antagonistic duality" of p21 in differentiation. Leuk Res **30:**1215-1216.
45. **Iordanskiy S, Waltke M, Feng Y, Wood C.** 2010. Subtype-associated differences in HIV-1 reverse transcription affect the viral replication. Retrovirology **7:**85.
46. **Nowak DE, Tian B, Jamaluddin M, Boldogh I, Vergara LA, Choudhary S, Brasier AR.** 2008. RelA Ser276 phosphorylation is required for activation of a subset of NF-kappaB-dependent genes by recruiting cyclin-dependent kinase 9/cyclin T1 complexes. Mol Cell Biol **28:**3623-3638.
47. **Kanazawa S, Peterlin BM.** 2001. Combinations of dominant-negative class II transactivator, p300 or CDK9 proteins block the expression of MHC II genes. Int Immunol **13:**951-958.
48. **Charles S, Ammosova T, Cardenas J, Foster A, Rotimi J, Jerebtsova M, Ayodeji AA, Niu X, Ray PE, Gordeuk VR, Kashanchi F, Nekhai S.** 2009. Regulation of HIV-1 transcription at 3% versus 21% oxygen concentration. J Cell Physiol **221:**469-479.
49. **Aboul-ela F, Karn J, Varani G.** 1996. Structure of HIV-1 TAR RNA in the absence of ligands reveals a novel conformation of the trinucleotide bulge. Nucleic Acids Res **24:**3974-3981.

50. **Chen ZJ.** 2005. Ubiquitin signalling in the NF-kappaB pathway. Nat Cell Biol **7:**758-765.
51. **Nekhai S, Kumari N, Dhawan S.** 2013. Role of cellular iron and oxygen in the regulation of HIV-1 infection. Future Virol **8:**301-311.
52. **Tsimberidou AM, Alvarado Y, Giles FJ.** 2002. Evolving role of ribonucleoside reductase inhibitors in hematologic malignancies. Expert Rev Anticancer Ther **2:**437-448.
53. **Allouch A, David A, Amie SM, Lahouassa H, Chartier L, Margottin-Goguet F, Barre-Sinoussi F, Kim B, Saez-Cirion A, Pancino G.** 2013. p21-mediated RNR2 repression restricts HIV-1 replication in macrophages by inhibiting dNTP biosynthesis pathway. Proc Natl Acad Sci U S A **110:**E3997-4006.
54. **Kim YS, Kang KR, Wolff EC, Bell JK, McPhie P, Park MH.** 2006. Deoxyhypusine hydroxylase is a Fe(II)-dependent, HEAT-repeat enzyme. Identification of amino acid residues critical for Fe(II) binding and catalysis [corrected]. J Biol Chem **281:**13217-13225.
55. **Hoque M, Hanauske-Abel HM, Palumbo P, Saxena D, D'Alliessi Gandolfi D, Park MH, Pe'ery T, Mathews MB.** 2009. Inhibition of HIV-1 gene expression by Ciclopirox and Deferiprone, drugs that prevent hypusination of eukaryotic initiation factor 5A. Retrovirology **6:**90.
56. **Hanauske-Abel HM, Saxena D, Palumbo PE, Hanauske AR, Luchessi AD, Cambiaghi TD, Hoque M, Spino M, Gandolfi DD, Heller DS, Singh S, Park MH, Cracchiolo BM, Tricta F, Connelly J, Popowicz AM, Cone RA, Holland B, Pe'ery T, Mathews MB.** 2013. Drug-Induced Reactivation of Apoptosis Abrogates HIV-1 Infection. PLoS One **8:**e74414.
57. **Yuan S, Zhang X, Lu L, Xu C, Yang W, Ding J.** 2004. Anticancer activity of methoxymorpholinyl doxorubicin (PNU 152243) on human hepatocellular carcinoma. Anticancer Drugs **15:**641-646.
58. **Gordeuk VR, Delanghe JR, Langlois MR, Boelaert JR.** 2001. Iron status and the outcome of HIV infection: an overview. J Clin Virol **20:**111-115.

843 **Fig.1. Effect of iron chelators on cellular iron and cell cycle progression.** (A) Chemical
844 structures of the Dp44mT, Bp4eT and Bp4aT are shown. (B-D) General steps for the synthesis
845 of PPY (control) and PPYeT and PPYaT iron chelators are shown. (E-G). Nano LC-FTMS
846 analysis of PPY, PPYeT and PPYaT. TIC, total ion current; EIC, extract ion chromatogram; PA,
847 peak area. As shown in EIC, PPY could be also detected in the samples of PPYeT and PPYaT.
848 The purities of PPYeT and PPYaT were 85% and 90% correspondingly.
849
850 **Fig.2 Effect of iron chelators on cellular iron and cell cycle progression.** (**A**) Labile iron pool
851 depletion. THP-1 cells were treated with 25 μM Ferric Sulfate for 1 hour at 37ºC, and then
852 loaded with 0.1 μM calcein-AM for 10 min at 37ºC. After washing with PBS, cells were treated
853 with 30 μM SIH, 3 μM PPY, 3 μM PPYeT or 3 μM PPYaT. Calcein fluorescence was measured
854 in real-time PCR Roche 4800 machine as a function of time. Fractional fluorescence $(F-F_0)/F_0$
855 proportional to the amount of chelatable iron was plotted on the Y axis. (**B**). Expression of
856 transferrin receptor (TFR) was measured in THP-1 cells treated with PPY-based iron chelators,
857 the non-chelating PPY compound and DMSO as control. RNA was extracted, reverse transcribed
858 and analyzed by real-time PCR using 18S RNA as normalization control. (**C-E**). Effect of PPY-
859 based iron chelators on the cell cycle progression. THP-1 cells, CEM T cells or 293T cells were
860 treated with 1 μM iron chelators for 24 hours and then fixed with 70% ethanol, stained with
861 propidium iodide (PI) and analyzed by FACS. Data were analyzed using BD FACS Calibur.
862 software. All results are shown as a mean of three independent measurements ±SD; asterisks
863 indicate $p \leq 0.01$.
864

865 **Fig.3. Inhibition of one round HIV-1 replication and toxicity in CEM T cells and PBMCs.**
866 **(A** and **C**). CEM T cells (panel A) or peripheral blood mononuclear cells (PBMCs) activated
867 with PHA and IL-2 (panel C) were infected with VSVG-pseudotyped pNL4-3.Luc.R-E- (HIV-1
868 Luc) virus for 18 hour at 37^{o}C and then treated for 24 hours at 37^{o}C with the indicated
869 concentrations of iron chelators. Then the cells were lyzed and luciferase activity was
870 measured. EC_{50}s were determined with GraphPad Prizm 6 Software. (**B**)**.** CEM T cells were
871 treated with the indicated concentrations of iron chelators for 24 hours at 37^{o}C. CEM T cells
872 were treated with 0.4 μM calcein-AM for 30 min and calcein fluorescence was measured at 485
873 nm excitation and 515 nm emission on the luminescence spectrometer equipped with the robotic
874 arm (Perkin Elmer LS 50B). EC_{50}s were determined with GraphPad Prizm 6 Software. (**D**).
875 Activated PBMCs were treated with the indicated concentrations of iron chelators for 24 hours at
876 37^{o}C and viability of cells was measured by trypan blue exclusion method. CC_{50}s were
877 determined with GraphPad Prizm 6 Software.
878
879 **Fig.4. Effect of PPY-based iron chelators on HIV-1 transcription in acutely and chronically**
880 **infected T cells and PBMCs.** (**A**). Treatment of the T cells acutely infected with subtype B
881 isolate of HIV-1 reduces viral transcription. A2R5.7 cells were incubated with NL4-3 strain of
882 HIV-1 (100 ng of p24 per ml) for 6 h at 37°C. Then the cells were washed twice with RPMI-
883 1640 medium, incubated with fresh culture medium containing indicated doses of PPY or PPYaT
884 for 48 h and harvested for RNA extraction and subsequent quantitative RT-real-time PCR with
885 the gag-specific primers. Results are shown as a mean of three independent measurements ±SD;
886 doubled asterisks indicate $p \leq 0.01$. (**B**) The T cells acutely infected with subtype C isolate of
887 HIV-1 displays dose-dependent effect on viral transcription. The A2R5.7 cells were inoculated

888 with HIV1084i strain of HIV-1 as described in A. The total RNA isolated from cells after 48h of
889 incubation with indicated iron chelators was reverse transcribed and analyzed by real-time PCR
890 with the gag specific primers. Results are shown as a mean of three independent measurements
891 ±SD; asterisk indicates $p \leq 0.05$. (**C**). Iron chelators inhibit viral transcription in chronically HIV-
892 1 infected T cells in dose-dependent manner. The J1.1 T cells (chronically HIV-1 infected cells
893 derived from Jurkat cell line) were pre-incubated with cART cocktail (10 μM Lamivudine, 10
894 μM Emtricitabine, 10 μM Tenofovir, and 10 μM Indinavir) for 7 days to avoid HIV-1 replication
895 and reinfection. After doubled wash the cells were incubated in fresh culture media without
896 drugs for 24 h and then for 48 h with the indicated doses of iron chelators. Subsequent isolation
897 and quantitative analysis of HIV-1 RNA was performed as described in panel A. Results are
898 shown as a mean of three independent measurements ±SD; asterisk indicates $p \leq 0.05$; doubled
899 asterisks - $p \leq 0.01$. (**D**) The treatment with iron chelators inhibits HIV-1 transcription in acutely
900 infected PBMCs. The PBMCs from three different donors were inoculated with dual-tropic
901 HIV-1 strain 89.6 for 6 h and after doubled wash incubated in IL-2 supplemented RPMI medium
902 for 72 h. Then the cells were washed again and incubated with IL-2 containing medium
903 supplemented with indicated doses of iron chelators for 48 h. RNA was isolated from cell
904 lysates and analyzed as described in A. Results are shown as a mean of triplicated samples.
905 Asterisk indicates $p \leq 0.05$; doubled asterisks - $p \leq 0.01$.
906
907 **Fig.5. PPY-based iron chelators induce expression of IKBα and affects NF-κB cellular**
908 **distribution.** (**A**). 293T cells were treated with 10 μM PPY, PPYaT or PPYeT. DMSO was used
909 as vehicle control. After 24 hours treatment, RNA was extracted, reverse transcribed and
910 analyzed by real-time PCR for CDK2, cyclin A, cyclin E, HLA and IKBα using 18S RNA as a

housekeeping control gene. (**B**). 293T cells were treated as in panel A, then lysed in SDS-PAGE loading buffer, resolved on 10% SDS-PAGE and probed with antibodies against IKBα, phosphorylated IKBα and tubulin as loading control. Results were quantified using Image Quant Software. Data are representative of two independent experiments. Low panel, averages of two independent experiments are shown. (**C**) 293T cells were treated as panel A, then fixed and stained with primary antibodies against NF-κB p65 subunit and secondary FITC-linked antibodies. Photographs were taken on (Olympus IX 51) at 200X magnification and .the pictures were scored for the distribution of NF-κB localized only in cytoplasm or both in the nucleus and the cytoplasm. Average data from 6 separate fields are shown. (**D**). NF-κB p65 expressions were analyzed by resolving cytoplasmic and nuclear extracts on 10% SDS-PAGE and immunoblotting with antibodies against NF-κB p65 subunit and tubulin as loading control.

Fig.6. Iron chelators inhibit CDK2 activity but increase CDK9 activity. (**A**). 293T cells were seeded into a 6 well plate and treated with 10 μM PPY or PPY-based iron chelators for 48 hours. Cells were lysed, and CDK2 was immunoprecipitated using anti-CDK2 antibodies. Kinase assay was performed using histone H1 as a substrate. Lower panel shows quantification from two independent experiments. (B). 293T cells were treated with iron chelators as in panel A. CDK9 was precipitated from cell lysates using anti-CDK9 antibodies and incubated with recombinant Rb-CTF in the presence of (^{32}P) ATP. The reactions were resolved on a 10% SDS Tris-glycine gel and analyzed by immunoblotting (lower panel) or on Phosphor Imaging Device (upper panel). Quantification from the Phosphor Imager is shown. Lower panel shows average results from two separate experiments. Asterisks indicate $p \leq 0.01$.

Fig.7. Treatment with iron chelators reduces the large P-TEFb complex. 293T cells were treated with 10 μM PPY or PPY-based iron chelators and then extracted sequentially to obtain low salt and high salt extracts as described in Materials and Methods. Low salt extract contains larger P-TEFb complex (LC) and high salt extract – small P-TEFb complex (SC). Amount of material was normalized to the total protein amount in the extracts, resolved on 10% SDS-PAGE and analyzed by immunoblotting for CDK9, and cyclin T1. (**A**). Representative immunoblotting results. (**B-C**). CDK9 and cyclin T1 expression are shown as an average from two separate experiments. Asterisks indicate $p \leq 0.05$ and double asterisk - $p \leq 0.01$.

Fig.8. Effect of PPY-based iron chelators on HIV-1 mRNA expression, HIV-1 reverse transcription and basal HIV-1 transcription. (A-B) THP-1 cells were uninfected or infected with HIV-1 Luc and then untreated or treated with DMSO, AZT, 1 μM PPY control compound, 1 μM PPYeT or 1 μM PPYaT as indicated for 48 hrs (A) or 6 hours (B). RNA (A) or DNA (B) was extracted. RNA was reverse transcribed and analyzed with primers for HIV-1 *gag* and *env* genes by real-time PCR on Roche 4800 using 18S RNA as a reference. DNA was analyzed by real-time PCR on Roche 4800 using primers for early and late LTR and β-globin gene as a reference. (**C-D**). Effect of PPY-based iron chelators on basal HIV-1 transcription. 293T cells were transiently transfected with vectors contacting HIV LTR followed by the luciferase reporter (WT HIV LTR 2xNFκB 3xSP1 (panel C), HIV LTR 2xNFκB ΔSP1 (panel D), or HIV LTR ΔNFκB 3xSP1HIV-1 (panel E), see Materials and Methods for vectors details). For normalization, the cells were also co-transfected with GFP expressing vector. At 24 hours post transfection the cells were treated with 10 μM PPY-based iron chelators or PPY control for 24

hours. Then the cells were lyzed and luciferase activity was measured. GFP fluorescence was measured in parallel and used for normalization. Asterisks indicate $p \leq 0.01$.

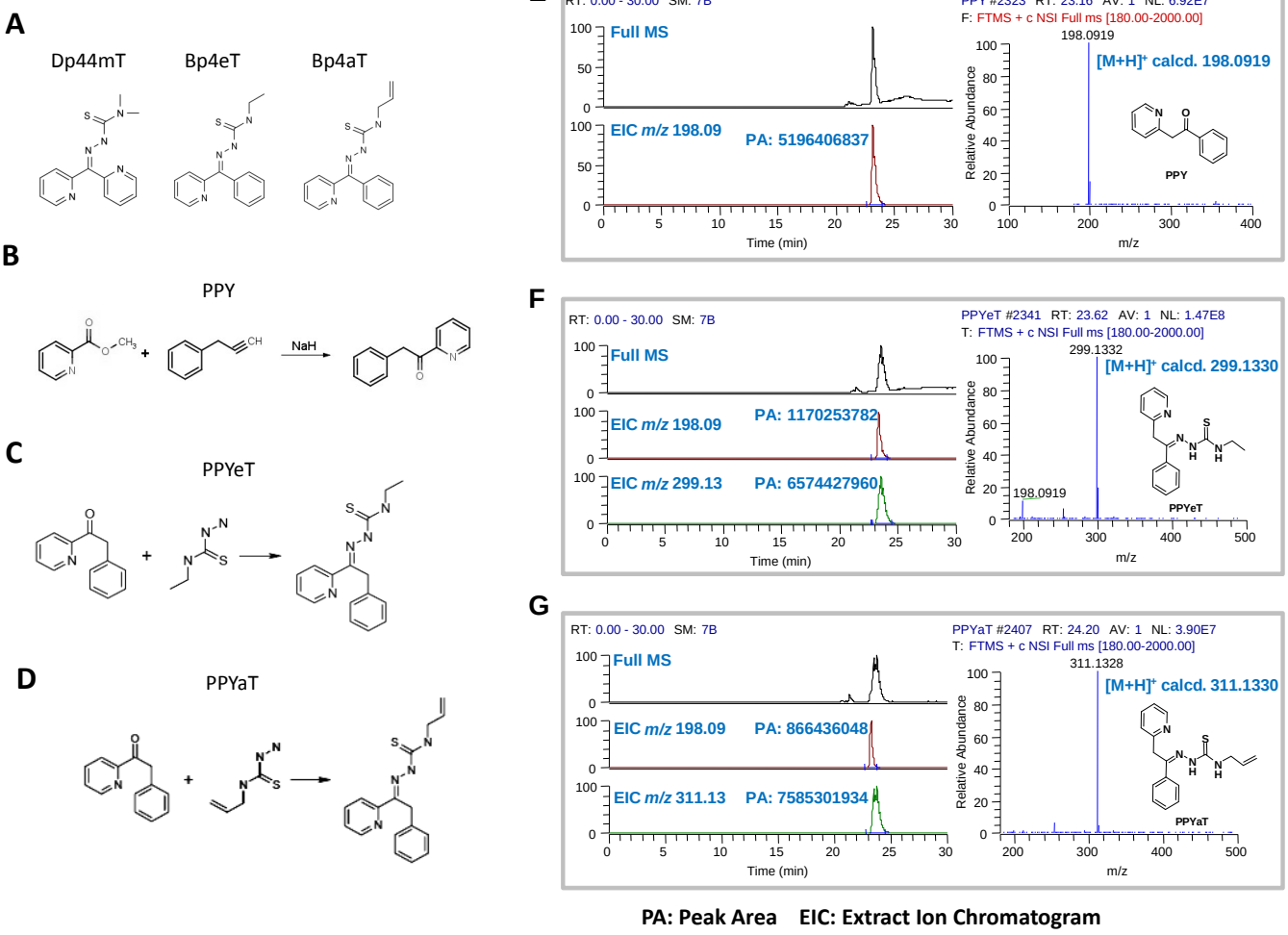

PA: Peak Area EIC: Extract Ion Chromatogram